Chem. Percept. (2008) 1:153–162
DOI 10.1007/s12078-008-9016-2

Role of Odorant Binding Proteins: Comparing Hypothetical Mechanisms with Experimental Data

Andrew J. Taylor · David J. Cook · David J. Scott

Received: 8 January 2008 / Accepted: 17 March 2008 / Published online: 13 May 2008

Abstract Odorant binding proteins are expressed in the olfactory epithelium of many mammalian species and are thought to assist in the uptake and transfer of odorants from the gas phase to the odor receptors. Various mechanisms have been proposed to explain how mass transfer occurs. Most experimental work has focused on the binding of ligands to odorant binding proteins or to the olfactory receptors under steady-state conditions, whereas the situation in vivo is dynamic due to the tidal flow of air through the nose and the mass transfer in and out of the olfactory epithelium. Some preliminary dynamic data have been obtained from an in vitro system, and this has been used, along with other published data, to test some of the proposed mechanisms for odorant binding protein (OBP). An assessment of the hypothetical mechanisms has been made to examine how well the mechanisms fit with the published experimental data. A new hypothesis is proposed where OBP acts to prolong the odor signal and increases the signal output of the olfactory system.

Keywords Mass Transfer · Ligand · Odorant · Release · Uptake · Model System · Olfaction · OBP

Introduction

Role of OBP

In vertebrates, odorant binding proteins (OBPs) are small (~20 kDa) soluble proteins of the lipocalin superfamily (Flower 1996) which are secreted in the nasal mucus at concentrations in the millimolar range. The significant conserved features of the lipocalins include a central hydrophobic cavity (the calyx) formed through an eight-stranded anti-parallel β-barrel, which can bind and transport hydrophobic molecules such as odorants. It is this functionality, together with the spatial expression (Hwang et al. 1988) and high concentration of OBPs in nasal mucus, which has led many researchers to suggest that they may play a direct role in olfaction. Rat OBPs have been studied in depth, and three forms have been isolated and their ligand-binding characteristics studied (Briand et al. 2000; Lobel et al. 2002; Nespoulous et al. 2004). These studies have concluded that the rat OBPs have a broad specificity, with each being tuned towards distinct chemical classes of odorants. Several hypotheses have been developed to explain the role of OBP in olfaction, and these are listed and described below.

The first hypothesis is that OBPs assist mass transfer of odorants from the gas to the liquid phase by solubilizing hydrophobic odorants in the nasal mucus layer. This process then facilitates the transport of odorants to the olfactory receptors (Pevsner and Snyder 1990). This might be described as the "universal solvent" hypothesis where the OBPs serve to compensate for the naturally low aqueous solubilities of many airborne hydrophobic odorants and make nasal mucus into a "universal solvent". In this paper, this mode of action is referred to as the "passive model of odorant binding" (PASMOB). Varying numbers of OBPs are found in different vertebrate species, and it is envisaged that the universal solvent functionality could be accomplished either by one or two OBPs with broad ligand specificities or by multiple OBPs where each OBP is more specifically tuned to a group of compounds or structural features. In this role, it has also been suggested that OBPs

A. J. Taylor (✉) · D. J. Cook · D. J. Scott
School of Biosciences, University of Nottingham,
Sutton Bonington Campus, Loughborough,
Leicestershire LE12 5RD, UK
e-mail: andy.taylor@nott.ac.uk

act as a specific filter, or the primary stage in odor coding, by actively binding certain compounds (Lobel et al. 2002; Steinbrecht 1998).

The second hypothesis is that the OBP–ligand complex facilitates uptake of ligand by the olfactory receptors (OR) in a so-called active process (ACTMOB). There is preliminary evidence of binding between OBP and one type of OR (Matarazzo et al. 2002), although the authors of the paper are wary of generalizing this finding to other ORs, and active transport of an odor ligand from OBP to OR has not yet been proven experimentally.

The third hypothesis is that OBPs act as an odorant scavenger or deactivator (DEACTMOB) by removing odorant from the olfactory receptors (Steinbrecht 1998). They therefore decrease "carry over" of odorant in the olfactory systems to prepare the system for the next odor stimulus, although there is no clear explanation of what happens to the odors after binding by OBP.

Studies on OBP

Due to their postulated role in olfaction, there has been considerable research interest in OBPs, and several have been extensively characterized, cloned, and purified in quantities which have enabled their ligand binding properties to be studied in vitro. One of the most widely used approaches has been to study the displacement of fluorescent probes from the OBP calyx (Pernollet and Briand 2004). Probes are selected which fluoresce only when they are in an apolar environment; hence, displacement of the probe from OBP by a preferentially bound ligand leads to a decrease in fluorescence intensity. Dissociation constants (K_d) may be calculated from a plot of fluorescence intensity against free ligand concentration. However, while such studies may be used to identify the structural features of molecules which facilitate binding to a particular OBP, it is not clear whether the relative affinities of binding to native OBPs can be inferred from the K_d values measured through competitive binding assays using fluorescent probes which are not found in nature.

A further technique which has been used to investigate ligand binding to OBPs is isothermal titration calorimetry (ITC; Nespoulous et al. 2004). This direct method for studying equilibrium binding requires a measurable enthalpy change upon binding. In such cases, ITC can be used to investigate the stoichiometry of binding and the affinity of OBPs for specific ligands.

The direct uptake of airborne odorants into solutions of OBPs has been demonstrated using volatile odorant binding assays (VOBA; Briand et al. 2000). These are equilibrium tests where odorant uptake into an OBP solution has been compared with that for an appropriate blank after a considerable time interval (>30 min). While the uptake of odorants at physiological concentrations (of OBP) supports the hypothesis that OBPs are involved in odorant transfer during olfaction, such experiments cannot be said to mimic the dynamic conditions which occur in vivo when odors are either inhaled or exhaled under conditions of turbulent flow in the nose. Moreover, all the techniques described above are steady-state studies where binding takes place over periods of minutes (1–30), whereas the situation in vivo involves the tidal flow of air over the nasal mucus every 5 s and results in a millisecond response to the odors (Laing et al. 1994). A sophisticated, dynamic mass transfer model of olfaction was described in 1994 (Hahn et al. 1994) but did not include a specific OBP binding step; instead, the overall mass transfer from air to mucus was considered.

Requirements for Dynamic Binding Studies

To date, no methods have been published for the study of dynamic binding of odorants to OBPs, meaning that their precise physiological role has remained a subject of speculation. In this paper, we describe a simple experimental apparatus to measure odorant binding to rat OBP-1 as a function of time. Rat OBP-1 was selected for these initial studies due both to its availability in a purified and highly characterized form and due to its relative stability compared to human OBP. A volatile laden gas flow, representative of aroma flowing over the olfactory epithelium, was bubbled through a solution of OBP (to achieve high surface area), and the concentration of odorant leaving the cell was monitored in real time using atmospheric pressure chemical ionization–mass spectrometry (APCI-MS). Thus, binding was monitored dynamically by following the depletion of aroma volatiles in the gas phase. The APCI-MS technique samples the gas phase at millisecond time intervals, enabling fast dynamic processes to be studied. Furthermore, as it is possible to monitor multiple ions simultaneously, the technique can be used to follow competitive binding in odor mixtures or the displacement of one odorant by a more tightly bound ligand. The aim of these studies was to provide information on some basic aspects of the initial steps in olfaction:

- How fast does rat OBP 1-f bind and release odor ligands?
- How easily is it saturated by an odor ligand?
- How is odor binding affected by the presence of other odor ligands presented either simultaneously or sequentially?

These simple studies led to a consideration of the physico-chemical conditions occurring during odorant uptake and, on this basis, a new hypothesis on the mode of action of OBP is proposed.

Materials and Methods

Materials

Rat OBP-1F was prepared by expressing a clone in *Pichia pastoris*, growing the yeast and isolating and purifying the protein as described previously (Briand et al. 2000). Solutions of OBP (0.175 to 3.5 mg/ml) were freshly prepared in phosphate-buffered saline (PBS buffer; 0.01 M phosphate, pH 7.4) and used within 1 day.

Odorants were obtained from Sigma Aldrich (Gillingham, UK) and known concentrations dissolved in water using a mechanical wrist shaker for 6 h (SF1; Stuart Scientific, Redhill, UK), followed by roller mixing (Stuart Scientific) overnight. The solutions were either placed in a sealed glass bottle, or in a glass syringe, to allow equilibration of the system, and the headspace was then used as the gas phase supply of odorant.

Bubble Through Apparatus

Apparatus consisted of a 4-ml glass vial (Sigma-Aldrich, UK) with a tapered conical base and sealed with a gas-tight septum. Two pieces of 530 μm fused silica capillary tubing were passed through the septum to allow the entry and exit of volatile-laden air. One piece extended to the vial base where gas was introduced. Gas exited through the second piece whose opening was located in the vial headspace, and the outflow was sampled into an APCI-MS (Thermo-Finnigan Deca LCQ Ion Trap MS) to monitor odorant concentration in the headspace as a function of time. Known concentrations of aroma compounds in air were delivered to the apparatus from a vertically mounted 100-ml gas-tight syringe (SGE Analytical Science, Milton Keynes, UK) containing 20 ml of an aqueous aroma solution at the appropriate concentration. Headspace from the syringe was pumped through the vial using a syringe pump (Harvard Apparatus, MA, USA); flow rates were 6 or 3 ml/min. The APCI-MS was set to sample the gas phase at rates just greater than those at which aroma was delivered (i.e., 7 and 4 ml/min), and the septum was additionally pierced with a fine hypodermic needle so that air could be drawn into the vial as a "make up" gas.

Two experimental paradigms were investigated. In the first, gas flow through the empty vial was maintained until a steady-state aroma concentration was monitored in the outflow using the APCI-MS. At this point, 0.5 ml of either OBP in buffer or buffer alone (control) was injected into the vial so that the gas flow now bubbled through the solution, and the impact of this on odorant concentrations was subsequently monitored for periods of several minutes. In the second configuration, the OBP/buffer or buffer solution was placed in situ in the vial before the delivery of aroma. In this configuration, the OBP could be loaded with one aroma compound and then "challenged" with another by switching flow between syringe pumps loaded with different odorants.

APCI-MS Analysis

Gas from the vial was sampled through 530-μm silica tubing into an APCI source via a heated transfer line (105 °C) and odorants ionized using a 5 kV corona discharge. Relevant operating conditions for the Thermo-Finnigan Deca LCQ Ion trap MS were: capillary temperature=200 °C; capillary voltage=3.0 V; tube lens offset=−35.0; max inject time 50 ms; scan range m/z 30:200. The MS output showed odorant ion intensity as a function of time, and this was converted into concentrations by introducing odorant calibrants (Linforth and Taylor 2003).

Calculation of Bubble Separation

The volume of the liquid in the vial was 0.5 ml and, as the bubble was formed from a 530-μm tube, the bubble radius was estimated as lying between 0.265 and 0.5 mm. The volume of gas in the liquid at any one time was estimated between 2% and 20% of the liquid volume (0.01 to 0.1 ml). From these values, the number of bubbles formed from a particular bubble radius and volume of gas in the liquid phase was calculated. It was then assumed that this number of bubbles occupied the total volume in the vial (the liquid plus the gas volume at any one time). It was assumed that the bubbles occupied the minimum volume due to close packing of the spheres, and therefore, the bubbles occupied 0.74048 of the total volume (Weisstein 2002). From these values, the radius of spheres to fill the volume was obtained and, after subtraction of the initial radius, the bubble separation was calculated and the values are shown in Table 1.

Table 1 Average distance (mm) between bubbles in the bubble through system

Bubble radius (mm)	Volume of gas in liquid at any one time (ml)			
	0.01	0.02	0.05	0.1
0.265	1.758	1.380	0.966	0.671
0.3	1.993	1.568	1.107	0.786
0.5	3.335	2.640	1.912	1.444

Values were estimated for different bubble sizes and gas volumes in the liquid phase. Assumptions made are detailed in "Materials and Methods"

Results and Discussion

Dynamic Binding Studies

The system developed for the dynamic binding studies was first used to measure the uptake of odorants in buffer and in buffer/OBP solutions. Figure 1 shows a typical trace obtained with ethyl butyrate. Initially, the air in the empty vial was replaced by a flow of ethyl butyrate (50 μl/l air) and the outflow from the vial monitored by APCI-MS. When the headspace concentration reached a steady state, an aliquot of buffer (or OBP in buffer) was injected into the vial and the gas flow containing the ethyl butyrate then bubbled through the liquid phase. The decrease in headspace concentration denoted uptake by the liquid phase. Rapid uptake was evident in both the buffer and buffer/OBP samples over the first 2 min with a slowing thereafter. Uptake by buffer was significant, but binding of ethyl butyrate to OBP/buffer was greater. It must be remembered that by measuring the volatile concentration in the gas phase, the uptake of ethyl butyrate by buffer and OBP is proportional to the area contained within the curve. In this experiment, the small disturbances in uptake noted in the first 30 s were attributed to the way in which the gas and liquid phases mixed as bubble flow was established in the initial stages of the experiment. Experiments were carried out with other volatile compounds and similar traces were observed. These experiments demonstrated the feasibility of the system for following dynamic binding of odorants to OBP and the necessity of measuring buffer uptake as a control for each set of experiments.

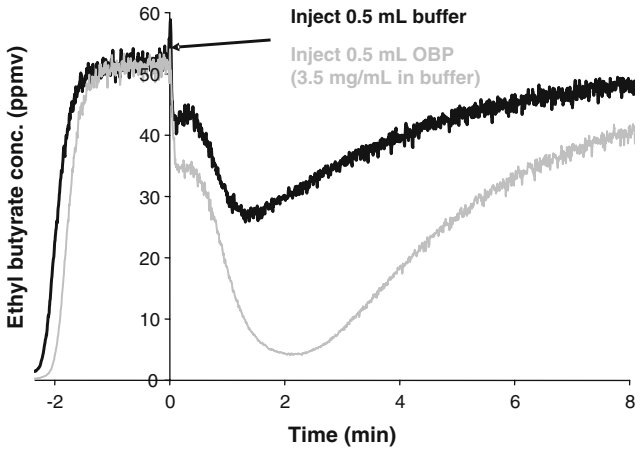

Fig. 1 Uptake of ethyl butyrate (50 μl/l air) by buffer and buffer/OBP. A gas flow of 6 ml/min was introduced into the apparatus and the headspace concentration monitored by online APCI-MS until it became steady (time −2 to 0 min). At time 0, an aliquot of OBP solution (0.5 ml containing 3.5 mg/ml of rat OBP-1) was introduced and the headspace concentration of the system monitored to follow the uptake of ethyl butyrate by the liquid phase

The speed and extent of binding of ethyl butyrate to OBP can be seen in Fig. 1. Under the experimental conditions used, there was an initial rapid uptake for about 1.5 min followed by a slower rate, presumably because the concentration difference between the gas and liquid phases became smaller and the "driving force" for mass transfer became less. It is also interesting to note that full saturation of the OBP/buffer system was not achieved in Fig. 1 (saturation would be denoted by the monitored headspace concentration returning to the original 50 μl/l headspace level). Calculations demonstrated that there were 94.5 nmol of OBP in solution (assuming rat OBP-1F has a MW of 18,500; Briand et al. 2000) and, over the 8-min period, 107 nmol of ethyl butyrate was delivered. Thus, in this system, binding was not quantitative, although attainment of saturation logically depends not only on the relative amounts of odorant and OBP but also on flow conditions in the system.

Further experiments were carried out to study the release rate after binding. Figure 2 shows the concentration of linalool in the headspace with time at three different gas phase concentrations of linalool. For the first 5 min, the system was loaded with 1, 5, or 25 μl/l linalool; thereafter, clean gas was introduced. Figure 2 shows the binding and release behavior using a normalized headspace concentration scale to allow easy comparison of the binding behavior at different linalool concentrations. The rate of release in this system is governed by the dissociation constant (K_d) of the (OBP + O) complex, the mass transfer of odorant through the liquid phase to the interface, and the partition coefficient. It is not easy to identify the rate limiting step from the data in Fig. 2 only to comment on the overall process assuming various scenarios. If linalool was very rapidly released (unlikely as the K_d values of OBP-ligand complexes show relatively tight binding), an initial increase in headspace concentration might be expected followed by a rapid decay to zero. If release was slow, then the headspace concentration would be expected to fall, as the small amounts released would be diluted by the flow of gas through the system. Instead, little change in headspace concentration was observed, suggesting that the rate of release is intermediate and that OBP is "buffering" the concentration in the headspace. This suggestion will be discussed later in the context of the role of OBP in olfaction.

Dynamic competition for OBP by odorants can also be studied using the bubble through system. Whereas the previously used fluorescent probe technique relies on dislodging a common probe from OBP (Briand et al. 2000), the APCI-MS monitoring system allows competitive binding between multiple odorant ligands to be studied and the speed of displacement noted. Figure 3 shows an example of odorant competition for OBP where 2-isobutyl-3-methoxypyrazine (IBMP) introduced in the gas phase

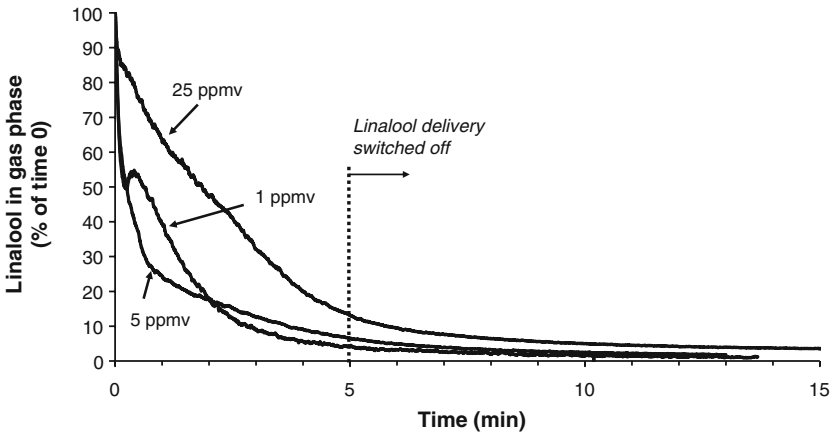

Fig. 2 Uptake and release of linalool at different gas phase concentrations. Linalool was delivered at 6 ml/min to a solution of OBP (for 5 min), then clean gas was bubbled through the OBP solution. Linalool concentrations have been normalized to the initial gas phase concentrations (100%) to compare the rates of uptake and release

displaces the citronellal already bound to OBP. Indeed, as soon as IBMP is introduced, citronellal appears in the headspace. Further experiments can obviously be carried out to determine the order and speed of displacement.

The brief experimental results above demonstrate that the bubble through system can give data on the rate and extent of odorant binding to OBP as well as show the temporal aspects of odorant competition for OBP. This represents a step forward over the VOBA assay (determined under equilibrium conditions) and the fluorescent probe assay (which only considers mass transfer in a liquid system). However, it is well established that mass transfer of odorants from the gas to the liquid phase depends very much on the timescale and length scale over which mass transfer processes (diffusion, convection, partition) occur. The relevance of the dynamic data obtained from the bubble through system compared to the situation in vivo needs further consideration, and these aspects are considered in the discussion below.

Discussion

Mass Transfer Processes

Figure 4 is a schematic representation of idealized odorant mass transfer from a liquid phase containing dissolved odorant to a gas phase containing no odorant. Dilution of the headspace by a flow of clean gas removes odorant from the gas bulk phase and provides a "pull" for the transfer of odorant through the other phases. In the bulk phases, mass transfer occurs by diffusion, convection, or turbulence (caused by stirring of the bulk phases). In the boundary layers, mass transfer is mainly mediated by diffusion and, at the interface, it is assumed that instantaneous partition occurs (deRoos and Wolswinkel 1994; Taylor 1998). The liquid boundary layer has more effect on mass transfer than the gas boundary layer (Marin et al. 2000), and the contribution of the latter layer has been ignored in the following discussion. Estimates of liquid boundary layer

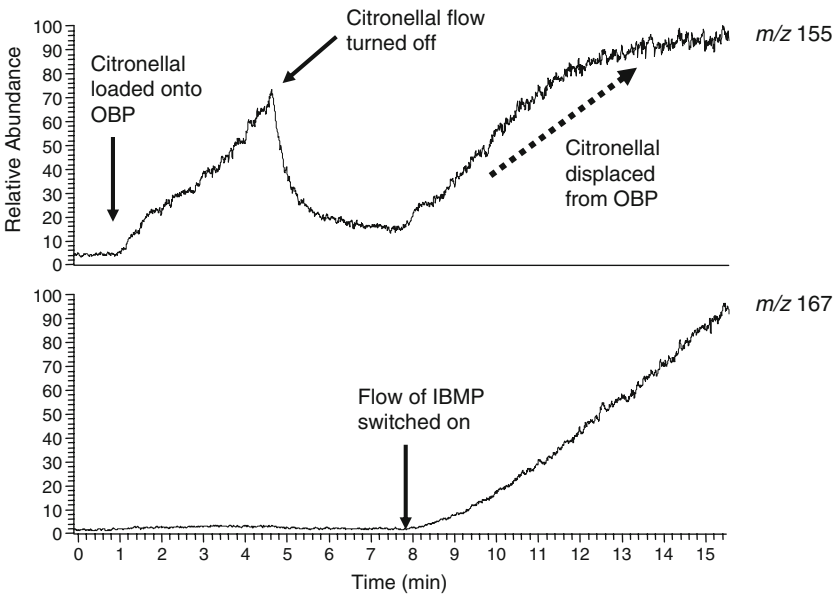

Fig. 3 Competition for OBP binding between citronellal and isobutylmethoxypyrazine (*IBMP*). The trace shows the raw data from the APCI-MS set for *m/z* 155 (top trace, corresponding to $[M+H]^+$ ion of citronellal) and *m/z* 167 (bottom trace, corresponding to IBMP $[M+H]^+$). Citronellal in air (5 μl/l) was bubbled through a solution of OBP (0.5 ml of a 0.175 mg/ml solution in PBS buffer) from 1.5 to 4.5 min and then replaced by clean air until 7.8 min when IBMP at 5 μl/l was bubbled through the citronellal loaded OBP. Immediate displacement of citronellal by IBMP can be seen

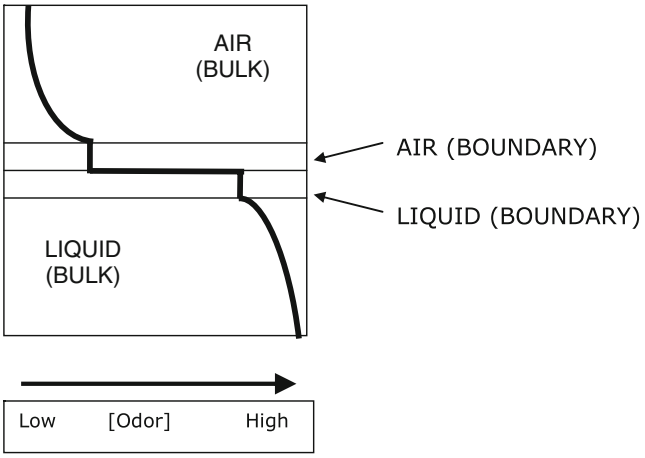

Fig. 4 Schematic of mass transfer of odorants between the gas and liquid phases showing the relative odorant concentration in the phases

thickness were obtained for a viscous, aqueous biopolymer system (1% carboxymethylcellulose) and water (Taylor 2002) from a release model proposed by de Roos and Wolswinkel (1994). Values for the liquid boundary layers were 3.8 and 28 μm, respectively, and these values could be taken as representative of the boundary layers in a viscous film (such as mucus) and in pure water (the situation from which most of the diffusive data has been obtained).

The next task was to compare these values with those for the in vitro bubble-through system and the situation in vivo.

Length Scales and Mass Transfer Mechanisms In Vitro

Several assumptions have to be made to estimate the path length that odor compounds have to travel from the gas to the liquid phase in the bubble-through system so that the random process of bubble flow through the liquid phase can be described by mathematical and physical principles. The first assumption is that the bubbles have a fixed, mean diameter and that at any one time, there is a certain volume of gas bubbling through the liquid phase. From these two values, the number of bubbles in the liquid at any one time can be calculated. Next, we propose that we fill the entire volume of the liquid with this number of bubbles and calculate the "filling diameter". Subtracting the radius of the actual bubble from the filling radius and multiplying by two will give a measure of average bubble separation. As the bubbles were formed from a 530-μm diameter tube, the radius is assumed to be a minimum of 0.265 μm, and observation of the change in overall volume in the bubble through system suggested a value between 2% and 20%. With a liquid volume of 0.5 ml, the gas volume at any one time was estimated between 10 and 100 μl. From this range of values, the average distance between bubbles was calculated, and Table 1 shows the values for bubble separation. The values lay between 670 and 3,335 μm or two to three orders of magnitude greater than the boundary layer values of 3.8 μm reported for a viscous solution. The conclusion is that in the bubble through system, mass transfer is occurring under bulk phase conditions, as the length scale is way outside the boundary layer conditions calculated for classical gas–liquid mass transfer. The next question was to determine the length scales over which mass transfer occurred in vivo.

Length Scales and Mass Transfer Mechanisms In Vivo

The thickness of the olfactory mucus layer is between 5 and 30 μm for frog olfactory epithelium (Menco and Farbman 1992), but the cilia on the OR cells are about 50 μm long (Farbman 2002) and appear as mats of overlapping fibers, suggesting that the mass transfer path in vivo must approach the boundary layer thicknesses. The consequence is that mass transfer in vivo almost certainly occurs through the boundary layer model and that diffusion and partition are the mechanisms for mass transfer. As partition is assumed to be instantaneous, diffusion must control the time needed for an odorant to cross the boundary layer. Using physico-chemical principles, this time can be estimated and compared with the known reaction times for odorant recognition (Laing et al. 1994) to confirm if the proposal of boundary layer mass transport is valid.

Values for diffusion times of different compounds can be found in theoretical texts (Crank et al. 1981) from which it is clear that diffusion times depend very much on length scales. The data of Crank et al. (1981) calculate the time for a molecule to diffuse a certain distance from a plane source in pure water at 25 °C, and diffusion times for a compound with a diffusion coefficient of 10^{-6} cm^2 s^{-1} (typical of an aroma compound in water) are 1 ms for a 1-μm distance, 10 s for 100 μm, and 1.7 days for 10,000 μm. Given the fact that odor recognition occurs in the hundreds of millisecond range, it follows that diffusion must occur over a distance of a few μm. However, the Crank data assume diffusion occurs in pure water and at a standard temperature of 25 °C, whereas the nasal mucus is more akin to a biofilm. Data taken from the Biofilms Hypertextbook (Cunningham and Ross 2007) estimate the time taken for 90% of a solute (t_{90}) to travel to the base of a biofilm of different thicknesses (L) using the equation $t_{90} = 1.03\frac{L^2}{D_e}$ where D_e is the effective diffusion coefficient in the biofilm. This equation is relevant to mass transfer in the nose, as it considers 90% of the odorant load and takes into account the fact that the diffusion coefficient changes depending on the nature of the aqueous environment (e.g., viscosity and temperature). For organic compounds related to odorants, the relationship between D_e for a biofilm and D_{aq} is around 0.29 (Stewart 1998), and to correct from the standard 25 °C temperature used for D_{aq} to nasal mucus

temperature (37 °C), a correction factor of 1.339 needs to be applied (Cunningham and Ross 2007). To obtain estimates of diffusion time through thin biofilms, values for benzene and propionic acid were calculated, as they represent hydrophobic and hydrophilic odorants (log P values 2 and 0.27, respectively). Both compounds have similar D_{aq} values (10.2 and 10.6, respectively; Cunningham and Ross 2007). To obtain values for D_e, the calculation is $D_{aq} \times 0.29 \times 1.339$, so D_e for both compounds is about 4×10^{-6} cm^2 s^{-1}. Substituting this value into the t_{90} equation above, the times for 90% of the odorant to move through a biofilm are 166 ms for L=5 μm, 27 ms for L=2 μm, and 6.6 ms for L=1 μm.

The calculations above assume that mucus can be represented as a regular slab with fixed dimensions. However, the olfactory receptors are located on cilia, some of which are motile (Mair et al. 1982). Unlike the nasal cilia, which move in a synchronous manner to encourage a flow of mucus through the nasal passages, the olfactory cilia show more random behavior until they are stimulated by odorants when they show jerky behavior initially, followed by "a crude metachronal synchrony" after 1 min (Mair et al. 1982). Translating this biological behavior into mass transfer terms, the movement of the cilia is likely to reduce the effective diffusion path length for odorants and thus speed mass transfer. The synchronous movement may assist removal of odorant from the mucus after the stimulus is removed. Modeling such behavior is extremely complex and is difficult to include in a mass transfer model. However, when interpreting experimental data, this fact should be considered, as it may confound the simple schemes presented here.

Although the values obtained above are estimates and based on certain assumptions, the inescapable fact is that if diffusion is the key mass transfer mechanism, then the path length for diffusion in vivo must be of the order of 1–5 μm for the transfer time to match the perceptual recognition values in the literature. For instance, the recognition time for propionic acid was quoted as 680 ms (Laing and Macleod 1992), which represents the time from administration of odorant at the nostril to the time when the panelist could recognize the odor as propionic acid, a process that involves a long sequence of chemical and neural processes. The conclusion from the comparisons of the systems in vitro and in vivo is that mass transfer in vivo is almost certainly a boundary layer process with a thickness around 1–5 μm but that the bubble through in vitro system involves mass transfer across longer distances (several hundred to several thousand μm, depending on the actual bubble size). Therefore, dynamic data from the bubble through system can provide comparative data on odorant OBP binding but are not representative of the situation in vivo, and a better model system needs to be developed.

Application of Data to Hypothetical Models of OBP

The simple schematic of odorant mass transfer in Fig. 4 can now be simplified, as the bulk phases can be disregarded and partition and diffusion will be the key mechanisms. The value of the partition coefficient depends on the solutes in the liquid phase as well as the physical conditions in the gas phase (laminar or turbulent flow; Marin et al. 1999, 2000). K_{gl} values are typically between 10^{-2} and 10^{-5}, meaning that for every one molecule in the gas phase, there are 100 or 100,000 molecules in the liquid phase, respectively. Therefore, if molecules in the gas phase encounter a liquid mucus phase containing no volatile molecules, mass transfer will readily occur from the gas to the liquid mucus phase until equilibrium is reached. The concentration of odorant in the liquid phase (O_l) will be determined by the gas phase concentration (O_g) as well as the K_{gl} value for that particular odorant. If boundary layer conditions exist in the mucus, mass transfer will be very rapid, so any change in gas phase odorant concentration should be followed by a change in the liquid phase odorant concentration within a period of 100–200 ms. If the situation is reversed and the odorant flux is from the liquid to the gas phase, one might expect equally rapid release of odorant (Eq. 1).

$$O_g \rightleftharpoons O_l \tag{1}$$

From the diffusion calculations above, most odorants are expected to have diffusion coefficients in the same order of magnitude, and thus, the diffusion time of the compounds will be very similar. Partition, on the other hand, is highly dependent on the hydrophobicity of the molecule, and aroma compounds show a wide range of partition coefficients spanning two to three orders of magnitude. Therefore, the extent of mass transfer between the phases will depend on the partition coefficient.

Considering first the DEACTMOB concept, it is difficult to rationalize this model with the idea that mass transfer across the gas–liquid interface is rapid (due to the boundary layer conditions), and the odorant will rapidly disappear from the liquid phase as soon as the odorant concentration in the gas phase decreases. There seems to be no advantage in OBP scavenging odorant from the liquid phase if the whole system is under boundary layer conditions and mass transfer is occurring rapidly in both directions. The notion that OBP scavenges odorant directly from the OR after the perceptual event is also difficult to explain, as this would involve either some OBP–OR interaction (see the ACT MOB discussion) or a mechanism to transfer odorant from OBP to OR and back again. The transfer would depend on the relative K_d values for OBP and OR, and it is not easy to explain how an effective two-way process could be accommodated.

The next step is to consider how OBP might affect mass transfer, and Eq. 2 shows the pathways involved.

$$O_g \underset{K_{gl}}{\rightleftharpoons} O_l \xrightarrow[OBP]{K_d} \{OBP + O\}_l \tag{2}$$

Given that the first part of the pathway is driven by partition, then OBP will initially bind the odorant in the liquid phase (O_l) and draw more odorant through the partition process as it attempts to restore equilibrium. The outcome is that the flux of odorant will increase from left to right in Eq. 2 with more odorant present in the bound (OBP + O) form. The concentration of O_l will depend on the balance of the partition and OBP binding kinetics but will either remain constant or decrease slightly. This result demonstrates why the ACTMOB hypothesis is attractive as OBP will increase the flux of odorant uptake and increase the concentration of the (OBP + O) complex. It is proposed that this complex then interacts with the ORs and transfers odorants from OBP to OR as shown in Eq. 3.

$$O_g \rightleftharpoons O_l \xrightarrow[OBP]{} \{OBP + O\}_l \xrightarrow[OR]{} \{OR + O\}_l + OBP \tag{3}$$

While this ACTMOB model has some attractions in terms of the mass flux through the first two steps of the process, the final part of the mechanism requires that OBP can interact with all of the ORs (about 350 in the human at the present time) and transfer the odorant ligands. Currently, the evidence for OBP–OR interaction is limited, with one paper reporting some functionality (Matarazzo et al. 2002). This mechanism is also incompatible with reports that odorants in aqueous solution can effectively interact with ORs in the absence of OBP (Firestein et al. 1993). Thus, despite its attractions, the ACTMOB model does not fit with the available experimental data.

Analysis of the published literature on the relationship between odorant concentration and the signal from ORs shows interesting behavior. There is certainly a dose–response behavior, i.e., the output of OR systems increases as the concentration of odorant increases, but there is also evidence that output can be affected by the *duration* of the stimulus applied. The results of Firestein et al. (1993) show that when a stimulus is presented at the same intensity, but for different time durations, the output signal from the OR system shows not only an increase in duration but also an increase in intensity (Fig. 5). The result is that an increase in stimulus duration amplifies the output signal. A similar result was reported when studying the administration of odors to subjects and monitoring brain activity using a PET scan (Hummel and Kobal 2002). Again, prolonging the duration of the signal caused an increase in both duration and intensity of the signal measured in the brain. Another example of stimulus duration shaping the response of biological systems can be found in the patterning of olfactory and lens tissue by bone morphogenetic protein (Sjodal et al. 2007). This latter example suggests that the concept of stimulus intensity and duration in the control of biological systems is a generic feature and not just confined to odor stimuli.

These phenomena suggest that both the concentration and persistence of odorant in the liquid phase could affect the output from ORs, and the role of OBP needs to be reassessed to incorporate this concept. Equation 4 proposes a mechanism where OBP has two functions. It increases the flux of odorant from left to right and then acts as a reservoir of odor so that when the concentration of O_l decreases as the gas phase concentration decreases, the system will react to maintain the concentration of O_l and increase the

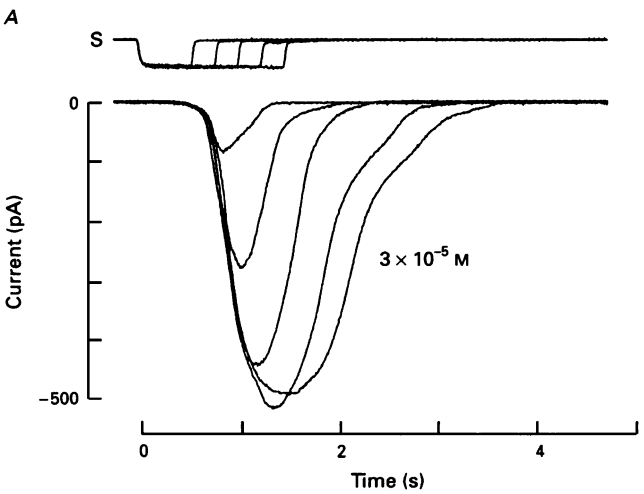

Fig. 5 Data showing the output of a salamander olfactory receptor cell (current in picoamps) subjected to a constant intensity stimulus but applied to the cell over different time durations (the trace labeled *A* shows the stimulus intensity and duration). Duration of stimulus increases both duration and intensity of the OR output. Reproduced from Journal of Physiology—London, 1994; *468*, 1–10 with permission

duration of the odor stimulus. This prolonged duration of the stimulus could therefore potentially increase the output signal from the OR system.

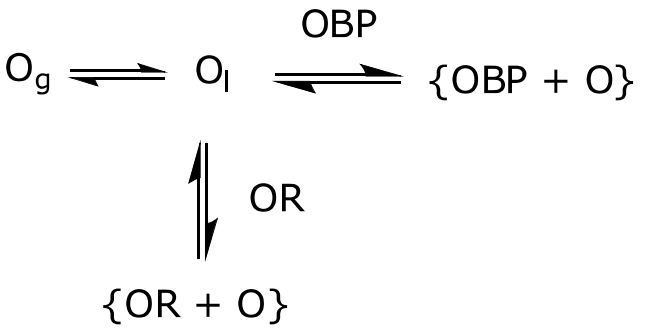

(4)

This mechanism does not require OR–OBP interaction and fits in with the existing experimental data. The data from the bubble through system when odorant was switched off showed that OBP exerted a "buffering" effect and maintained the gas phase concentration at a fairly constant level as the OBP unloaded. This provides some supporting evidence for the mechanism in Eq. 4, albeit from a system operating on a different length scale to that found in vivo.

Conclusion

It is proposed that mass transport of odorants from the air in the nostril to the olfactory receptors located in the olfactory epithelium occurs under boundary layer conditions. The hypothesis is supported by direct measurements and observations of frog olfactory epithelium as well as through calculations of the time needed for odorants to move through the system which indicate a layer thickness of 1–5 μm. The times are consistent with the observed times for odorant recognition. With this information, the various hypotheses on the role of OBP were evaluated and a new hypothesis proposed which fits the experimental evidence available. To understand the dynamics and mechanisms of odorant transport, a bubble through model system was developed and tested. While the model system delivered improved information on odorant binding and competition for OBP, the length scale was still two to three orders of magnitude greater than the situation in vivo. New model systems are needed to understand how the in vivo system operates and which physico-chemical parameters are key in the uptake and release of odorants in the olfactory epithelium.

Acknowledgments We thank Loic Briand and Jean-Claude Pernollet (INRA Jouy-en-Josas, France) for generously supplying OBP and helping in setting up OBP production in our laboratory as well as discussing the merits of the different OBP binding assays. An anonymous reviewer helpfully suggested the idea of ciliary action and its potential effect on mass transfer. The UK research council, BBSRC, provided funding for the practical part of the project.

References

Briand L, Nespoulous C, Perez V, Remy JJ, Huet JC, Pernollet JC (2000) Ligand-binding properties and structural characterization of a novel rat odorant-binding protein variant. Eur J Biochem 267 (10):3079–3089

Crank J, McFarlane NR, Newby JC, Paterson GD, Pedley JB (1981) Diffusion processes in environmental systems. Macmillan, London

Cunningham AB, Ross RJ (2007) The Biofilms Hypertextbook. Retrieved 23 December 2007

deRoos KB, Wolswinkel K (1994) Non-equilibrium partition model for predicting flavour release in the mouth. In: Maarse H, Van der Heij DG (eds) Trends in flavour research. Elsevier Science, Amsterdam, pp 15–32

Farbman AI (2002) Olfactory organs of vertebrates. In: Finger TE, Silver WL, Restrepo D (eds) The neurobiology of taste and smell, 2nd edn. Wiley-Liss, New York

Firestein S, Picco C, Menini A (1993) The relation between stimulus and response in olfactory receptor-cells of the tiger salamander. J Physiol (Lond) 468:1–10

Flower DR (1996) The lipocalin protein family: Structure and function. Biochem J 318:1–14

Hahn I, Scherer PW, Mozell MM (1994) A mass-transport model of olfaction. J Theor Biol 167(2):115–128

Hummel T, Kobal G (2002) Olfactory event-related potentials. In: Simon SA, Nicolelis MAL (eds) Methods in chemosensory research. CRC, Boca Raton

Hwang PM, Pevsner J, Sklar PB, Venable JC, Snyder SH (1988) Localization of rat odorant-binding protein to the lateral nasal gland suggests an odorant transport function. Chem Senses 13 (4):699–699

Laing DG, Macleod P (1992) Reaction time for the recognition of odor quality. Chem Senses 17(3):337–346

Laing DG, Eddy A, Francis GW, Stephens L (1994) Evidence for the temporal processing of odor mixtures in humans. Brain Res 651 (1–2):317–328

Linforth RST, Taylor AJ (2003) Direct mass spectrometry of complex volatile and non-volatile flavour mixtures. Int J Mass Spectrom 223–224:179–191

Lobel D, Jacob M, Volkner M, Breer H (2002) Odorants of different chemical classes interact with distinct odorant binding protein subtypes. Chem Senses 27(1):39–44

Mair RG, Gesteland RC, Blank DL (1982) Changes in morphology and physiology of olfactory receptor cilia during development. Neuroscience 7(12):3091–3103

Marin M, Baek I, Taylor AJ (1999) Flavour release from aqueous solutions under dynamic headspace dilution conditions. J Agric Food Chem 47:4750–4755

Marin M, Baek I, Taylor AJ (2000) Flavor release as a unit operation: a mass transfer approach. In: Roberts DD, Taylor AJ (eds) Flavor release, vol 763. American Chemical Society, Washington, DC, pp 153–164

Matarazzo V, Zsurger N, Guillemot JC, Clot-Faybesse O, Botto JM, Dal Farra C et al (2002) Porcine odorant-binding protein selectively binds to a human olfactory receptor. Chem Senses 27(8):691–701

Menco BPM, Farbman AI (1992) Ultrastructural evidence for multiple mucous domains in frog olfactory epithelium. Cell Tissue Res 270(1):47–56

Nespoulous C, Briand L, Delage MM, Tran V, Pernollet JC (2004) Odorant binding and conformational changes of a rat odorant-binding protein. Chem Senses 29(3):189–198

Pernollet J-C, Briand L (2004) Structural recognition between odorants, olfactory-binding proteins and olfactory receptors—first events in odour coding. In: Taylor AJ, Roberts DD (eds) Flavor perception. Blackwell, Oxford, pp 86–150

Pevsner J, Snyder SH (1990) Odorant-binding protein—odorant transport function in the vertebrate nasal epithelium. Chem Senses 15(2):217–222

Sjodal M, Edlund T, Gunhaga L (2007) Time of exposure to bmp signals plays a key role in the specification of the olfactory and lens placodes ex vivo. Dev Cell 13:141–149

Steinbrecht RA (1998) Odorant-binding proteins: expression and function. In: Olfaction and taste XII. New York Academy of Sciences, New York, vol 855, pp 323–332

Stewart PS (1998) A review of experimental measurements of effective diffusive permeabilities and effective diffusion coefficients in biofilms. Biotechnol Bioeng 59(3):261–272

Taylor AJ (1998) Physical chemistry of flavour. Int J Food Sci Technol 33(1):53–62

Taylor AJ (2002) Release and transport of flavours in vivo: physico chemical, physiological and perceptual considerations. Comprehensive Reviews in Food Safety and Food Science 1:45–57

Weisstein EW (2002) CRC concise encyclopedia of mathematics, 2nd edn. CRC, Boca Raton